Continuous-Discrete Systems – Modelling and Statistical Analysis

Jörg Krupar, Andreas Mögel and Wolfgang Schwarz

Faculty of Electrical Engineering and Information Technology, Dresden University of Technology
Mommsenstr. 13, 01069 Dresden Germany
Email: {krupar/moegel/schwarz}@iee1.et.tu-dresden.de

Abstract—Continuous-discrete or hybrid systems have experienced a growing interest by various researchers over the last decade. They serve as models for applications in modern electronics and control engineering. In this paper a basic model of continuous-discrete systems is provided. It covers a variety of systems of practical use. For simple continuous subsystems switching schemes are introduced and discussed in a systematic manner. For the case of chaotically working systems a statistical analysis, i.e. the estimation of statistical characteristics of the output signal is treated. The methods presented can be directly used for the analysis and design of power electronic systems such as charge pumps, DC-DC converters and switching motor drivers. The paper has tutorial character.

1. Introduction

Hybrid systems are common parts in modern electronic systems [1]. They consist of a continuous subsystem and a discrete subsystem, see Fig. 1. The discrete subsystem
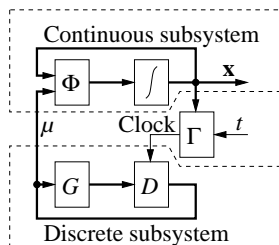

Figure 1: Hybrid system.

consists of an iterated map G and a delay unit D. The state equation is

$$\mu_{n+1} = G(\mu_n) \,. \tag{1}$$

The continuous subsystem consists of an integrator block and a static analog part Φ. It is described by the state equation

$$\frac{d\mathbf{x}}{dt} = \Phi(\mathbf{x}, \mu) \,. \tag{2}$$

The function Γ defines the switching conditions from the time t and the state $\mathbf{x}$. It is represented by a manifold in the $x - t$ space (Fig. 2). Fig. 3 depicts two inportant special cases the pure time or horizontal control and pure event or vertical control. A control scheme consisting of a mix of pure time conditions and pure event conditions appears in
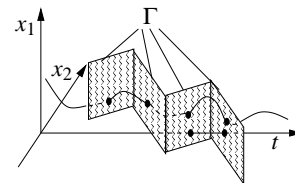

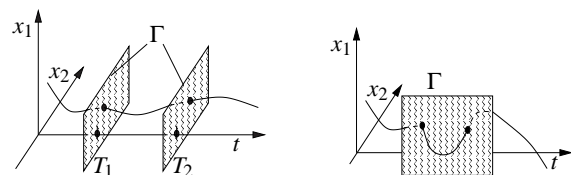Figure 2: Mixed time – event control.

Figure 3: Time and event control.

DC-DC converters. We note that this is also a special case of Fig. 2.

In the analysis of hybrid systems often some approximation is possible that allows to reduce the order of the system. The case of one-dimensional systems is investigated in the sequel.
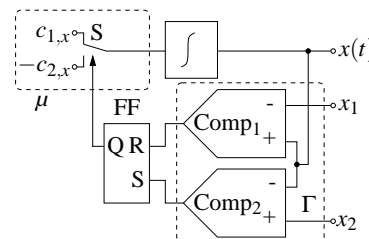
2. One-Dimensional Systems

Figure 4: Vertical control.

Fig. 4 depicts a vertically controlled system. Depending on the output Q of the flip-flop the switch S applies the value c_1 or $-c_2$ to the integrator and the state $x(t)$ decreases or increases linearly with time. When $x(t)$ exceeds x_1 the Flip-Flop is reset by Comp_1 and when $x(t)$ falls below x_2 the Flip-Flop is set by Comp_2. Vertical switching schemes always include a state feedback.

A horizontally controlled system is depicted in Fig. 5. The switch is controlled by a sequence of control times $t_{1,n}$
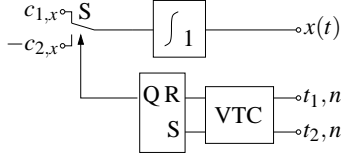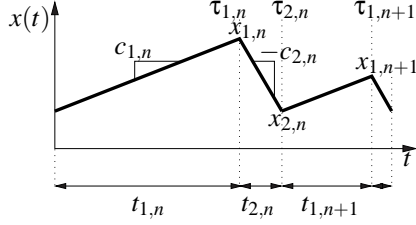
Figure 5: Horizontal control.

Figure 6: State trajectory.

and $t_{2,n}$. They can be generated by a value to time converter (VTC). The VTC can be realised e.g. by Fig. 4.

Tab. 1 summarises the state trajectories and the maps of vertical and horizontal control. The ocurrence times of set and reset events are

$$
\begin{aligned}
\tau_{1,n} &= \tau_{2,n-1} + t_{1,n} \\
\tau_{2,n} &= \tau_{1,n} + t_{2,n} .
\end{aligned}
\tag{3}
$$

A third control scheme is slope control (Tab. 2). Here the sequence of the slopes $\mathbf{c}_n = \begin{pmatrix} c_{1,n} \\ c_{2,n} \end{pmatrix}$ is generated by a return map $\mathbf{C}$ (Tab. 2). The switching instants can be controlled horizontally or vertically. Vertical control corresponds to frequency modulation (FM) and horizontal control corresponds to amplitude modulation (AM).

Both maps $\mathbf{G}$ and $\mathbf{H}$ in Tab. 1 have their special application in the analysis of hybrid systems as shown in Tab. 3

Often an equivalence is desired to derive $\mathbf{H}$ from $\mathbf{G}$ and vice versa. Because $\mathbf{H}$ includes difference information only

Table 1: Vertical and horizontal control.

$\mathbf{c}_{n+1} = C(\mathbf{c}_n)$	
	Vertical slope control (FM) $x_1 = const.$ $x_2 = const.$
	Horizontal slope control (AM) $t_1 = const.$ $t_2 = const.$

Table 2: Slope control schemes.

Hybrid system analysis	
Vertical map $\mathbf{G}$	Horizontal map $\mathbf{H}$
Bifurcation analysis Value control optimisation Density calculation	Power density spectrum Autocorrelation funktion

Table 3: Hybrid system analysis.

(no state feedback – see Fig. 5) this is not possible in general. However in our case of a piecewise linear state-time function a conversion function

$$
\mathbf{t}_n = \mathbf{K}(\mathbf{x}_n)
\tag{4}
$$

can be found that allows to extract horizontal values from the sequence of vertical control values and vice versa. Three important special cases are discussed in the next section.

3. Special control schemes

Constant upper value	Constant lower value
$g_1(\mathbf{x}) = x_1$ $g_2(\mathbf{x}) = g(x_2)$	$g_1(\mathbf{x}) = g(x_1)$ $g_2(\mathbf{x}) = x_2$
$k_1(\mathbf{x_n}) = \frac{x_1 - x_{2,n}}{c_1}$ $k_2(\mathbf{x_n}) = \frac{x_1 - g(x_{2,n})}{c_2}$	$k_1(\mathbf{x_n}) = \frac{x_{1,n} - x_2}{c_1}$ $k_2(\mathbf{x_n}) = \frac{x_{1,n} - x_2}{c_2}$

Table 4: Constant limit vertical control, [1], [2], [3].

Firstly we consider two control schemes where the upper or lower switching level is constant. Tab. 4 depicts these

56

cases and shows the corresponding conversion function (4). Both schemes are used in DC-DC converters (current programmed mode). They generally have the disadvantage that the mean value m depends on the map $\mathbf{G}$ and hence $\mathbf{G}$ interferes with the value control if the constant x_1 or respectively x_2 is used as correcting variable.

To overcome this problem another control scheme that has not been published yet to our knowledge is introduced in Tab. 5. It uses a constant mean value and the upper and lower limits vary symmetrically with respect to the mean value. The difference z_n between the upper and lower limit is generated by a return map g. It is ideal for this purpose
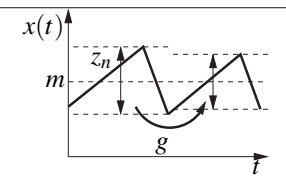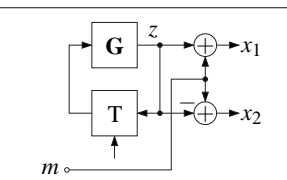
Control scheme	Realisation
$z_{n+1} = g(z_n)$	
$x_{1,n} = m + z_n$	$k_1 = \frac{z_{n-1} + z_n}{c_1}$
$x_{2,n} = m - z_n$	$k_2 = \frac{2z_n}{c_2}$

Table 5: Symmetrical control scheme.

as z is the modulation input that is independend from the mean value. Hence value control and modulation do not interact. The scheme is realised by combining the scheme of Tab. 5 with the system in Fig. 4.

For the slope controlled case the conversion function is summarised in Tab. 6. As the slopes c_1 and c_2 are deter-

$\mathbf{c}_{n+1} = G(\mathbf{c})$	
Vertical slope control	Horizontal slope control
$k_1(\mathbf{x}) = \frac{x_1 - x_2}{c_1}$	$x_{1,n} = x_{2,n-1} + c_{1,n}t_1$
$k_2(\mathbf{x}) = \frac{x_1 - x_2}{c_2}$	$x_{2,n} = x_{1,n} - c_{2,n}t_2$

Table 6: Slope control schemes.

mined by the converters input and output voltages this control scheme is not applicable to DC-DC converters.

4. Statistical Analysis

4.1. Densities

Densities are used in the analysis of the static properties of the state signal $x(t)$. Let $f_{x_1}(x)$ and $f_{x_2}(x)$ be the densities of the upper limit x_1 and the lower limit x_2 respectively. Then the density of the signal $x(t)$ calculates as

$$f_x(x) = \frac{1}{\eta} \int_{-\infty}^x (f_{x_2}(y) - f_{x_1}(y)) \, dy \qquad (5)$$
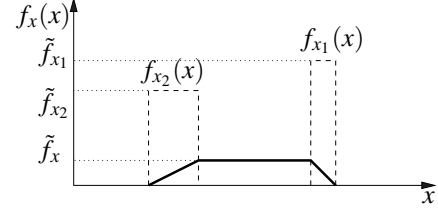

Figure 7: Value density, general case.

with the normalisation constant

$$\eta = \int_{-\infty}^\infty (f_{x_2}(y) - f_{x_1}(y)) \, dy \, dx = m_{x_1,1} - m_{x_2,1} \qquad (6)$$

i.e. the difference of the mean values of x_1 and x_2

Fig. 7 depicts an example where x_1 and x_2 are uniformly distributed.

From Eq. 5 we can directly derive the density of the special cases in Tab. 4. Constant upper value control results in

$$f_x(x) = \begin{cases} \frac{1}{\eta} \int_{-\infty}^x f_{x_2}(y) dy & x \le x_1 \\ 0 & x > x_1 \end{cases} \qquad (7)$$
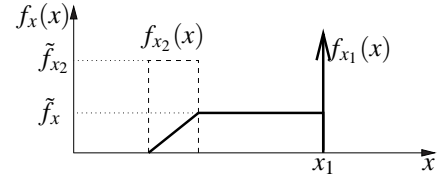

Figure 8: Value density, constant x_1.

Fig. 8 depicts the corresponding density when x_2 is uniformly dirtributed. The constant x_1 corresponds to a δ-density.

Constant lower value control results in

$$f_x(x) = \begin{cases} 0 & x \le x_2 \\ \frac{1}{\eta} \int_{-\infty}^x (1 - f_{x_1}(y)) dy & x > x_2 \end{cases} \qquad (8)$$

The shape of the density is obtained by mirroring Fig. 8 horizontally.

For the symmetrical control scheme of Tab. 5 the density is obtained by

$$f_x(x) = \frac{1}{\eta} \int_{-\infty}^x f_g(m - x) - f_x(x - m) dy \qquad (9)$$
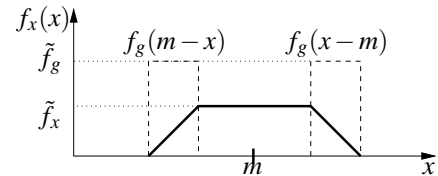
Fig. 9 shows an example.

Figure 9: Value density, symmetrical control.

4.2. Moments

From Eq. (5) we obtain for the nth moment of the signal $x(t)$

$$m_{x,n} = \frac{1}{n+1} \frac{m_{x_1,n+1} - m_{x_2,n+1}}{m_{x_1,1} - m_{x_2,1}} \ . \tag{10}$$

From this equation the moments for the special control schemes in Tabs. 4 and 5 can be derived. The result is

$$m_{x,n} = \frac{1}{n+1} \frac{1}{x_1 - m_{x_2,1}} (x_1^{n+1} - m_{x_2,n+1}) \tag{11}$$

for constant upper value control,

$$m_{x,n} = \frac{1}{n+1} \frac{m_{x_1,n+1} - x_2^{n+1}}{m_{x_1,1} - x_2} \tag{12}$$

for constant lower value control and

$$m_{x,n} = \frac{1}{n+1} \frac{m_{m+g,n+1} - m_{m-g,n+1}}{m_{2g,1}} \tag{13}$$

for the constant mean value control. The first and second moment of $x(t)$ are used for calculation of the mean value of $x(t)$ which is important for an outer control loop and the variance which gives the total AC power of this process which is important for EMI considerations.

4.3. Power Density Spectrum, [1], [3], [4], [5], [6]

The power density spectrum characterises the dynamics of the process $x(t)$. The signal $x(t)$ can be understood as a twicely integrated pulse process. Thus it can be modeled by a linear filtered pulse process (Fig. 10)
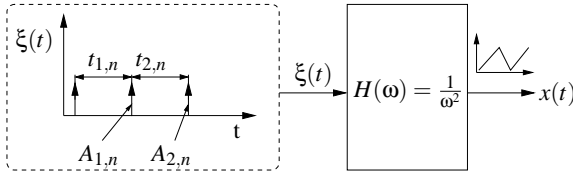

Figure 10: Pulse process model.

$$\xi(t) = \sum_{n=0}^{\infty} (A_{1,n}\delta(t - \tau_{1,n}) - A_{2,n}\delta(t - \tau_{2,n})) \ . \tag{14}$$

$A_{\cdot,n}$ are the pulse intensities

$$\begin{aligned} A_{1,n} &= -c_{1,n} - c_{2,n} \\ A_{2,n} &= c_{1,n} + c_{2,n} \end{aligned} \tag{15}$$

and $\tau_{1,n}$ and $\tau_{2,n}$ are the pulse occurence times from Eq. (3). The linear filter

$$H(\omega) = \frac{1}{\omega^2} \tag{16}$$

performs double integration. Its output power density spectrum is

$$S_x(\omega) = \frac{S_\xi(\omega)}{\omega^2} \ . \tag{17}$$

The power density spectrum of the pulse process is calculated by [5]

$$S_\xi(\omega) = \lim_{T \to \infty} \frac{1}{T} E\left(|F_T(\omega)|^2\right) \tag{18}$$

with

$$F_T(\omega) = \sum_{n=1}^{N(\xi,T)} A_{1,n}e^{j\omega\tau_{1,n}} - A_{2,n}e^{j\omega\tau_{2,n}} \ . \tag{19}$$

5. Conclusions

We have given an overview over control and analysis of hybrid systems. For one-dimensional systems we proposed a detailed library of control schemes. A new advantageous control scheme has been introduced. It allows the separation between value control and dynamical properties of the system.

Statistical analysis of one-dimensional piecewise linear in time systems has been presented. The results from previous work can be derived as special cases from the analysis results proposed.

Further generalisation of the analysis to other kinds of hybrid systems is due to future work.

References

[1] J. Krupar, A. Mögel and W. Schwarz"Analysis of Hybrid Systems by Means of Embedded Return Maps", *in Proc. ISCAS'04*, volume V, pp.656–659, Vancouver, 2004, Canada

[2] C. Tse"Tutorial Notes on Chaos in Power Electronics", ISCAS'03, Bangkok, 2003, Thailand

[3] A. L. Baranovski, A. Mögel, W. Schwarz, and O. Woywode"Chaotic control of a DC-DC-converter", *in Proc. ISCAS'00*, volume II, pp. 108–112, Geneva, 2000, Switzerland

[4] A. L. Baranovski and W. Schwarz"Chaotic and Random Point Processes: Analysis, Design and Application to Switching Systems", IEEE Trans. CAS I, vol. 50, pp.1081–1088, August 2003

[5] J. Krupar and W. Schwarz"Spread Spectrum Clock Generation – Chaotic and Periodic Modulation Schemes", *in Proc. ECCTD'03*, pp.235–238, Krakow, 2003, Poland

[6] J. Krupar, A. Mögel and W. Schwarz"EMI-Performance of DC-DC Converters – Criteria and Spectral Optimisation", *in Proc. NOLTA'04*,Fukuoka, 2004, Japan